# Quantum Mechanical Pulling Force Generation through Matter-Wave Impingement on Heterogeneous System

ROSHLAN RAHMAN DIPTO $^{1,*}$ , MIR SAKHAWAT HOSSAIN $^2$ , MD. ASIFUZZAMAN $^3$ , ABDUS SATTAR MOLLAH $^{1,*}$ 

Department of Nuclear Science and Engineering, Military Institute of Science and Technology, Dhaka, BANGLADESH
 <sup>2</sup>GIS Division, Center for Environmental and Geographic Information Services, Dhaka, BANGLADESH
 <sup>3</sup>Department of Electrical Engineering and Electronics, North South University, Dhaka, BANGLADESH
 \*Corresponding author's

Abstract: - The use of optical manipulations that changes the mechanical properties of light has been crucial across multiple fields. These techniques are being used in various optics and phonics applications. By following the same physical theory we can manipulate an atomic sized particle in the quantum domain. We have proposed an asymmetric configuration model to reverse quantum pulling force on a Xenon atom at a certain angle resulting from the interaction energy of the matter wave (Helium) near a copper substrate. Several full-wave quantum simulations and on this quantum mechanical configuration with two counter-propagating plane matter waves at different angles were performed. By utilizing a solution of time independent Schrödinger equation and stress tensor formula we calculated the force on the quantum particle. It implies physical adsorption scatterer phenomena that can be used for the development of modern quantum applications such as particle trapping and inertial confinement fusion.

Key-Words: - Optical, Manipulation, Quantum, Schrödinger, Phonics, Fusion, Substrate.

Received: May 12, 2025. Revised: June 13, 2025. Accepted: August 11, 2025. Published: October 24, 2025.

# 1 Introduction

In the two decades since the invention of optical trapping, which is popular as optical tweezers, a potential method has been demonstrated to have wide-ranging applications in both biology and physics. The capabilities of this method has progressed from basic manipulation to exert calibrated forces on optically trapped objects and measuring their displacements at the nanometer scale. In 1970, Ashkin introduced a physical mechanism in which the radiation pressure can accelerate and trap particles [1]. Later in 1986 he demonstrated a trapping method in which he utilized a single focused laser to manipulate dielectric particles [2]. In this study he highlighted that without any complex setup, gradient force from the

light's electric field can capture and stabilize nanoparticles. This concept became popular as optical trapping in 1986, which later resulted in him receiving the Nobel Prize in Physics in 2018. This is a well-known fact that light can exert radiation pressure on a particle to push towards the direction of propagation by momentum transfer. Recently macroscopic object manipulation by monochromatic light beams has achieved a new level of advancement in technology. Marston et al. investigated the axial radiation force by tuning the Bessel beam's half-cone angle  $(\theta)$ , sphere's size relative to the wavelength and the refractive index contrast between the particle and the surrounding medium [3]. Chen et al. explored counterintuitive optical pulling force where light exerts a net force that pulls a particle toward the source of photon

radiation pressure that pushes objects away [4]. Similarly Novitsky et al. demonstrated a new mechanism where a single gradientless beam can function as a tractor beam [5]. He showed that without relying on complex traditional intensity gradients, this approach exploits tailored momentum transfer and scattering dynamics to achieve net backward motion of particles along the beam axis. At first Brzobohaty et al. presented experimental realisation of an optical tractor beam which is capable of complex tasks like transporting, sorting and dynamically self-arranging particles using a single structured light field [6]. In addition, Qiu et al. demonstrated inhomogeneous dielectric mixtures which have varying optical properties can cause tractor beam effects by enabling photon momentum transfer [7]. This study made bridges between structured media engineering and optical forces, showing how fabricated dielectric environments can reverse conventional radiation pressure dynamics. Chen et al. presented the use of Fano resonance to induce a negative optical scattering force in plasmonic nanoparticles [8]. By manipulating interference between narrowband dipolar and broadband quadrupole plasmon modes can pull the particles toward the light source. Sadgrove et al. explored quantum optical manipulation mechanism for trapped atoms near a nano waveguide where atoms are pulled towards the light source through quantum interference and coherent light-matter interactions [9]. Krasnov et al. demonstrated almost the same thing by introducing a bichromatic optical tractor beam [10]. The properties of polarization or spin-projection are responsible for lateral force in the condition of circularly polarized light [11, 12]. The main objective of this research is manipulation of quantum objects like atoms or molecules at a certain angle. We have utilized here the Helium atom as a matter wave instead of light, similar to the optical trapping mechanism. It is quite similar to optical pulling force, quantum mechanical matter wave exerts pressure on an scatterer and pulls that object towards the direction of matter wave propagation. This incident occurs by interaction of the quantum matter wave with the metal surface that generates

reverse force on the atom. The whole setup is asymmetric.

# 2 Set-up Model and Method

A heavy atom is scattered in the presence of external surface energy by Helium atoms. The heavy atom is situated at a distance d from the metal surface. The origin of the coordinate system was defined on the center of the heavy atom. Two plane matter waves having the same energy on the heavy atom are impinged with a slope with X axis. Matter waves propagate from +X axis to -X axis. We have taken the Helium-4 as our incident particle, the Scatter as the atoms of the Xenon gas, and as a metal substrate Copper was chosen. We have applied several full wave based simulations. The simulation data was generated from d = 0.3 nm to d = 1 nm for 45° of the incident angle. Furthermore, three specific scenarios for d = 0.3 nm, d = 0.7 nm and d = 1 nm have been analyzed varying incident angle from 0° to 90°. Fig. 3 and 4 presents a generic view of the simulation setup.

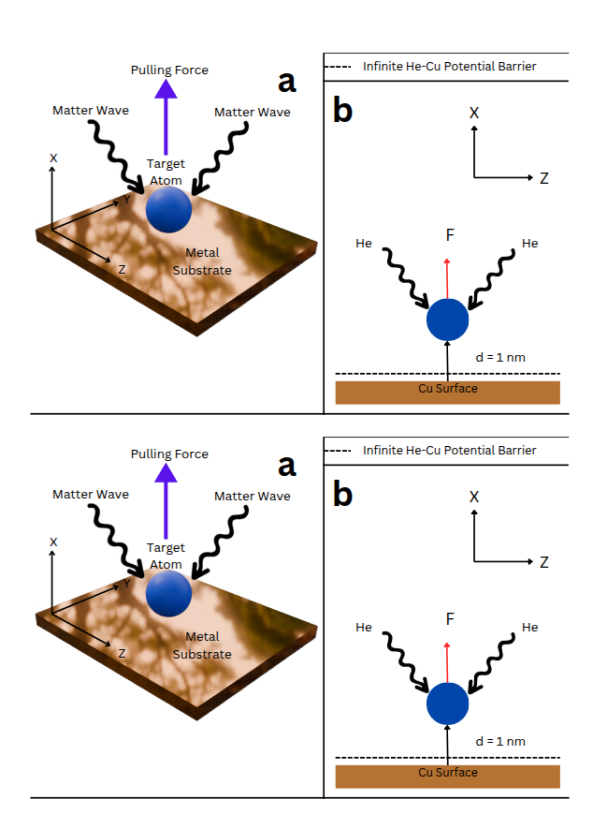


Fig 1: 3D Model of Optical Pulling Force Set-up. Here the Dash line denotes physisorption potential energy barrier. He Matter-wave was propagated from +X and -X axes. Quantum pulling force was found towards X-axis.

In contrast to Ref. [14], the Center of Mass reference frame is not applicable in our scenario due to the presence of an external force acting on the particles so we applied the laboratory reference frame. In the case of adsorption, the target atom vibrates with minimal vibrational energy, which causes low kinetic energy and no time-averaged momentum. If vibrational kinetic energy is neglected, the target particle can be approximated as motionless. For simplicity, we are taking the target atom to be motionless for all d. In the simulation, the Schrödinger equation was solved for the incident particles of the mass of the free particles that are scattered by the stationary scatterer and the metal surface. Throughout the entire system, a constant mass is assumed for the incident particle. The beam with thermal energy (25 meV) is taken initially for analysis and further analysis is performed with varying the energy of the incident beam. A stationary study was performed taking the potential energy independent of time and the energy of the incident particle as a fixed parameter. There are two types of potential energy in the whole set-up. One is the He-Cu potential energy and the other is the He-Xe potential energy.

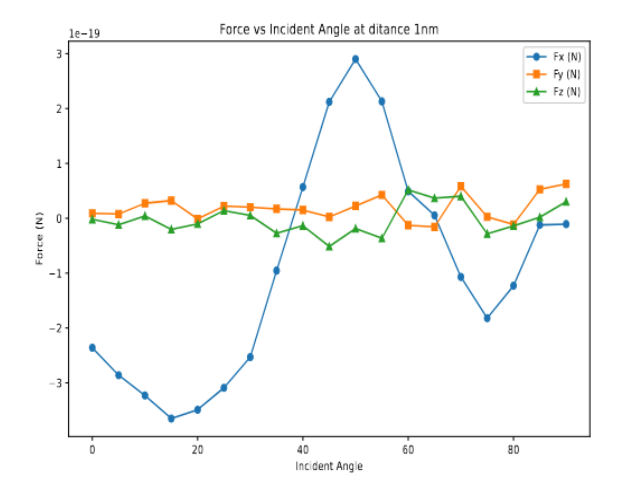


Fig 2: Force at Distance 1 nm plot

The energy of the He-Cu potential depends on the incident beam energy, Figure 1 was taken for all simulations with different incident beam energies. For the second part, the potential energy of Tang-Toennies is chosen [13]. The shape of the interaction is simplified by considering it to be a

step potential energy curve as a result the complexity of the calculation gets reduced, and it implementation of the quantum mechanical stress tensor [14] in COMSOL Multiphysics. Both the scalar potential energies as function of position were summed up as the Hamiltonian of a system. Time-independent potential energy is expressed by the sum of potential energy and kinetic energy of the incident beam. Shown in Figure 1 using QM stress tensor the time-averaged forces was calculated which is acting on the scatterer atom. In the direction of x,y and Z force density vectors were calculated and a surface integration was done at  $r = 9.1 \times BR$  distance which is slightly larger than the scatterer atom's radius to get the respective time-averaged force components acting on the particle. Any closed surface at a distance larger than  $9 \times BR$  can be used for surface integration since the He-Xe potential energy is negligible. In contrast to Ref. [14], the Center of Mass reference frame is not applicable in our scenario due to the presence of an external force acting on the particles so we applied the laboratory reference frame. In the case of adsorption, the target atom vibrates with minimal vibrational energy, causes low kinetic energy and no time-averaged momentum. If vibrational kinetic energy is neglected, the target particle can be approximated as motionless. For simplicity, we assume the heavy target particles as motionless across all other dimensions, given that they are approximately 32 times heavier than the incident particles and cold. Therefore, in our simulations, we solve the Schrödinger equation for the incident particles, which have the mass of free particles, under the influence of the stationary scatterer and the metal surface.

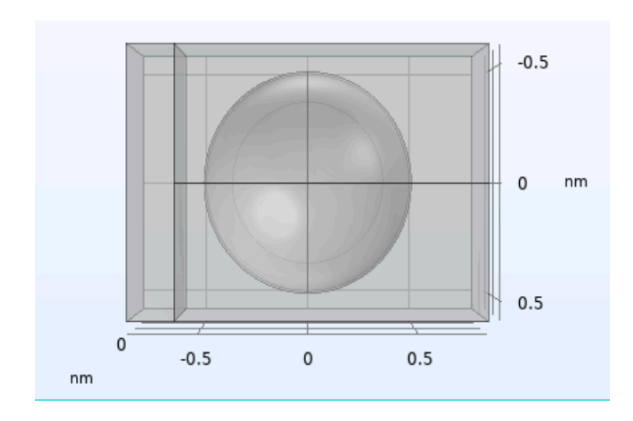


Fig 3: Geometry Setup in COMSOL

To model the setup, it is necessary to set the data including the free particle mass of the incident beam particles, and the total potential energy of the system and the energy E of the incident beam. The mass of the incident particle is assumed constant across the entire domain of the system. The beam's energy, set at 25 *meV*, is defined the same as Ref. [14], where a coherent beam with thermal energy at room temperature was generated using an energy selector. For further analysis, the energy ranges from 0 meV to 100 times of 25 meV.

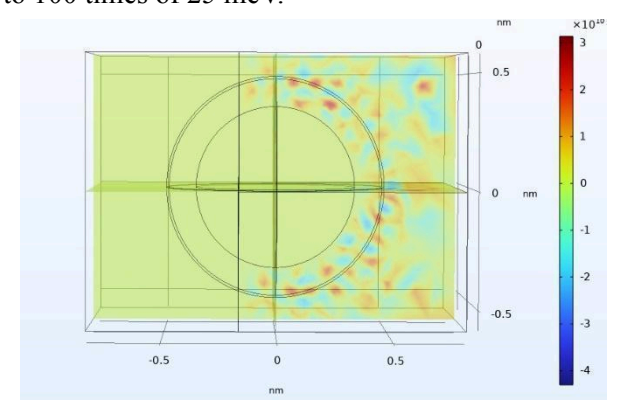


Fig 4: Post Processing in COMSOL

Since the potential energy is time-independent and the incident particle's energy is a fixed parameter, a stationary study could be experimented. Our whole set-up was divided into two parts of the potential energy. One is the interaction energy between the incident particles and the surface (He–Cu potential energy) and the other is the interaction energy between the incident particles and the scatterer (He–Xe potential energy). Values related to the potential values are tabulated in table 1.

**Table 1:** Simulation Parameters

Parameter Name	Notation	Value
Initial incident energy	Е0	1.87e-3 eV
Helium Mass	mHE	3.8462*amu
Potential Energy of Scatterer	U0	-37.7*E0
Wave Amplitude	A0	sqrt(10e20)

For the first component the shape of the interaction energy curve typically varies with the incident beam energy, and was used uniformly across all simulations. Here the attractive (long range) part was not affected due to the far distance between the adsorbate and surface. We have discussed impact of the impact of scaling the He-Cu potential energy in the Results and Discussion section. We did not find any significant variation in the magnitude of force. The trend of the force related to the distance between Xe and the infinite barrier of the He-Cu interaction energy aligned with theoretical prediction. It is discussed in the subsequent section. This agreement with analytical and simulated values are presented in table 2 in simulations across a broad range of incident beam energies where multichannel scattering does not occur because it is out of our scope. In this study we applied Tang-Toennies' potential energy [13]. To simplify the computational complexity and effective use of quantum mechanical (QM) stress tensor [14], the interaction is modeled using a step approximation of the potential energy curve. We computed force along X, Y and Z directions and applied greater than 9 times of Bohr radius for particles. According to Ref.[14] stress tensor can be derived by calculating expected value of force by incident particle in the total potential energy is:

$$F_{inc} = - \int \Psi^* \nabla U sc \, \psi dV \dots (1)$$

where  $F_{inc}$  is the force on the incident particle by the scatterer,  $\psi$  is the total stationary wave function and Usc is the potential energy of the incident particle

due to the scatterer. By solving time-independent Schrödinger equation (TISE) for the incident particle in the total energy of the system yields the wave function  $\psi$ :

$$\frac{-h^2}{2m}\nabla\psi + (Usurf + Usc)\psi = E\psi \dots (2)$$

where m means mass of incident particle, *Usurf* expresses potential energy of incident particle due to surface and E denotes the energy of incident beam. By simplifying we get from Equation 1 and Equation 2,

$$\psi * \nabla \psi = - \nabla \cdot \left[ \nabla I^2 \right] \dots (3)$$

We get,

$$F_{inc} = \int \vec{\nabla} \cdot \left[ \frac{h^2}{2m} (\vec{\nabla} \psi \otimes \vec{\nabla} \psi^* + \vec{\nabla} \psi^* \otimes \vec{\nabla} \psi) + \underline{I} \left( \left( E - U_{surf} - U_{sc} \right) |\psi|^2 + \frac{h}{2m} |\vec{\nabla} \psi|^2 \right) \right] dV$$

$$(4)$$

Because of momentum conservation during leaving the scatterer by incident particle it acts an opposite force Fsc on the scatterer. We write Fsc in terms of quantum stress tensor,

$$\langle F \rangle_{inc} = -\langle F \rangle_{sc} = -\left(-\oint \langle \overrightarrow{T} \rangle \langle \cdot \rangle d\overrightarrow{s}\right) = \oint \langle \overrightarrow{T} \rangle \cdot d\overrightarrow{s}$$
....(5)

Here  $\langle \rangle$  denotes time average of by applying divergence theorem we get,

$$T = \frac{\hbar^2}{2m} \left( \vec{\nabla} \psi \otimes \vec{\nabla} \psi^* + \vec{\nabla} \psi^* \otimes \vec{\nabla} \psi \right) + \underline{T} \left[ \left( E - U_{surf} \right) \cdot \right]$$
(6)

From Equation 5 and 6 we get,

$$\vec{F}_{sc} = -\frac{h^2}{2m} \left[ r^2 \oint \left( 2Re \left[ \vec{\nabla} \psi \left( \vec{\nabla} \psi^* \cdot \hat{n} \right) \right] \right) \cdot \hat{n} + \frac{2m \left( E - U_{swr} \right)}{h^2} |\psi|^2 - \left| \vec{\nabla} \psi \right|^2 \right] d\Omega$$
....(7)

where n is the outward unit vector, Fsc is the scattering force,  $\psi$  denotes the wave function of the incident He atom, Usurf is the surface potential, Usc potential energy of the incident particle, T is the stress tensor and h cut is the reduced planck's constant. Here we find that  $|Fsc| \propto |A|^2$ , A = By

applying quantum stress tensor method, we have compared the theoretical model with simulation results by running full wave simulation with COMSOL Multiphysics.

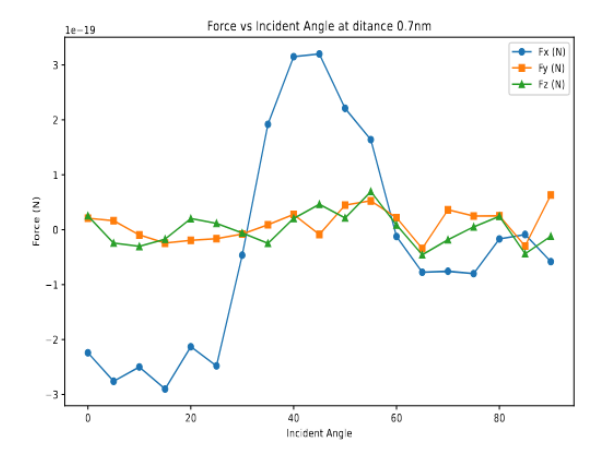


Fig 5: Force at distance 0.7 nm Plot

### 3 Result and Discussion

The set-up for simulation with an incident beam is shown in Fig. 1(a) where the scatterer feels force in the presence of a copper surface. Fig. 1(b), (c) and (d) show two incident beams are impinged on the scatterer making an angle with the Z axis. Fig. 1(c) shows that the scatterer feels no pushing force towards +X axis if the Copper surface is 0.3nm distant from the scatterer.

**Table 2** Theoretical and Simulation values of Force (N) at 0.7 nm

Angles (Degree)	Theoretical	Simulated
5	-2.8832E-19	-2.7582E-19
20	-2.03456E-19	-2.1256E-19
30	-4.5243E-20	-4.6356E-20
40	3.03423E-19	3.1488E-19
45	3.2571E-19	3.1968E-19
50	2.3456E-19	2.2111E-19
60	-1.00543E-20	-1.2305E-20
80	-1.546785E-20	-1.6777E-20

Fig 5 shows that pushing force turns out to be pulling when the copper surface is 0.7nm distant from the scatterer when the incident angle of both beams is 45° aligned with the X axis. We saw that the magnitude of pulling force for  $d = 7.0^{\circ}A$  should be  $1.46 \times 10-20N$ , which is very close to the lateral force obtained from the simulation  $3.6769 \times$ 10-19N. No pulling force was found to be experienced by the scatterer up to 0.6nm (see Fig 2 and 5). Maximum pulling force was found for 0.7nm see Fig 5. For 0.3nm, 0.7nm and 1nm force with angle variation were calculated. For 0.7nm from the incident beam making an angle with Z axis from 35°to 45°pulling force was observed and for 1nm from 40° to 65°. Fig 6 shows the dependency of force felt by the scatterer on the incident beam energy. For 40 times of 25meV we found the highest pulling force.

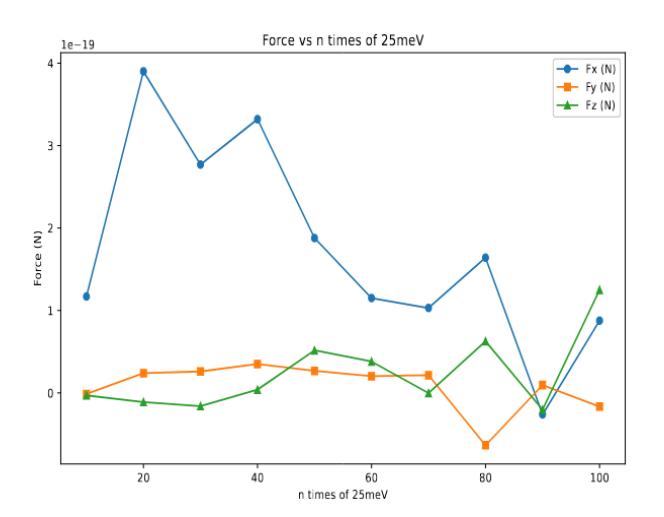


Fig 6: Force at Difference Energy

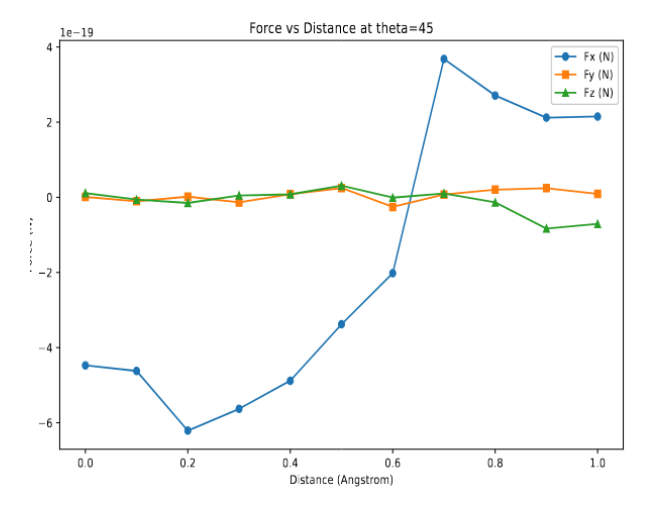


Fig 7: Force at different distance where  $\theta = 45^{\circ}$  plot

# 4 Conclusion

From the experiment, the existence of Quantum mechanical pulling force in presence of surface energy was achieved. From the configuration we found two different phenomena, while the target atom was so near the surface the target atom didn't feel any pulling force along the opposite direction of the incident of the matter wave though the incident angle was varied. The second scattering event was observed while the target atom was kept at some distance from the surface, for a particular range of incident angle of the matter wave the target atom showed to be pulled by the matter waves. A significant change in the value of force was found when energy of the incident matter wave was varied. Where any kind of background potential energy is involved and fields like laser trapped fusion, particle trapping these observations this manipulation can be further utilized. Further study can be done using spin dependency and electric charge involved systems.

#### 5 Ackwoledgement

The authors are thankful to the Department of Nuclear Science and Engineering at the Military Institute of Science and Technology for providing all the essential facilities.

#### **6 Author Contribution**

Roshlan Rahman Dipto - Data Acquisition, Resources, Conceptualization, Methodology Mir Sakhawat Hossain - Data analysis, Writing, Resources, Writing - Original Draft. Asifuzzaman - Data Acquisition, Resources. Abdus Sattar Mollah - Supervision, Resources, Review and Editing.

#### References:

- [1] Ashkin, A. (1970). Acceleration and trapping of particles by radiation pressure. *Physical Review Letters*, 24(4), 156–159. <a href="https://doi.org/10.1103/physrevlett.24.156">https://doi.org/10.1103/physrevlett.24.156</a>
- [2] Ashkin, A., Dziedzic, J. M., Bjorkholm, J. E., & Chu, S. (1986). Observation of a single-beam gradient force optical trap for dielectric particles. *Optics Letters*, *11*(5), 288. <a href="https://doi.org/10.1364/ol.11.000288">https://doi.org/10.1364/ol.11.000288</a>
- [3] Marston, P. L. (2006). Axial radiation force of a Bessel beam on a sphere and direction reversal of the force. *The Journal of the Acoustical Society of America*, 120(6), 3518–3524. https://doi.org/10.1121/1.2361185
- [4] Chen, J., Ng, J., Lin, Z., & Chan, C. T. (2011). Optical pulling force. *Nature Photonics*, 5(9), 531–534. <a href="https://doi.org/10.1038/nphoton.2011.153">https://doi.org/10.1038/nphoton.2011.153</a>
- [5] Novitsky, A., Qiu, C., & Wang, H. (2011). Single gradientless light beam drags particles as tractor beams. *Physical Review Letters*, 107(20). <a href="https://doi.org/10.1103/physrevlett.107.2036">https://doi.org/10.1103/physrevlett.107.2036</a>
- [6] Brzobohatý, O., Karásek, V., Šiler, M., Chvátal, L., Čižmár, T., & Zemánek, P. (2013). Experimental demonstration of optical transport, sorting and self-arrangement using a 'tractor beam.' Nature Photonics, 7(2), 123–127 <a href="https://doi.org/10.1038/nphoton.2012.33">https://doi.org/10.1038/nphoton.2012.33</a>
- [7] Qiu, C., Ding, W., Mahdy, M., Gao, D., Zhang, T., Cheong, F. C., Dogariu, A., Wang, Z., & Lim, C. T. (2015). Photon momentum transfer in inhomogeneous dielectric mixtures and induced tractor beams. *Light Science & Applications*, *4*(4), e278. https://doi.org/10.1038/lsa.2015.51
- [8] Chen, H., Liu, S., Zi, J., & Lin, Z. (2015). FANO Resonance-Induced negative optical scattering force on plasmonic nanoparticles.

- *ACS Nano*, *9*(2), 1926–1935. https://doi.org/10.1021/nn506835j
- [9] Sadgrove, M., Wimberger, S., & Chormaic, S. N. (2016). Quantum coherent tractor beam effect for atoms trapped near a nanowaveguide. *Scientific Reports*, 6(1). https://doi.org/10.1038/srep28905
- [10] Krasnov, I. (2012). Bichromatic optical tractor beam for resonant atoms. *Physics Letters A*, 376(42–43), 2743–2749. <a href="https://doi.org/10.1016/j.physleta.2012.07.0">https://doi.org/10.1016/j.physleta.2012.07.0</a>
- [11]Sukhov, S., Kajorndejnukul, V., Naraghi, R. R., & Dogariu, A. (2015). Dynamic consequences of optical spin–orbit interaction. *Nature Photonics*, *9*(12), 809–812. https://doi.org/10.1038/nphoton.2015.200
- [12] Rodríguez-Fortuño, F. J., Engheta, N., Martínez, A., & Zayats, A. V. (2015). Lateral forces on circularly polarizable particles near a surface. *Nature Communications*, 6(1). https://doi.org/10.1038/ncomms9799
- [13] Tang, K. T., & Toennies, J. P. (2003). The van der Waals potentials between all the rare gas atoms from He to Rn. *The Journal of Chemical Physics*, *118*(11), 4976–4983. https://doi.org/10.1063/1.1543944
- [14] Gorlach, A. A., Gorlach, M. A., Lavrinenko, A. V., & Novitsky, A. (2017). Matter-Wave tractor beams. *Physical Review Letters*, *118*(18). <a href="https://doi.org/10.1103/physrevlett.118.180401">https://doi.org/10.1103/physrevlett.118.180401</a>